First order sensitivity analysis of magnetorheological fluid damper based on the output damping force[①]

Kong Xiangdong(孔祥东)[＊][＊＊], Li Bin[＊], Quan Lingxiao[②][＊][＊＊], Guo Haixin[＊], Bai Ruxia[＊]

(＊College of Mechanical Engineering, Yanshan University, Qinhuangdao 066004, P. R. China)
(＊＊Hebei Provincial Key Laboratory of Heavy Machinery Fluid Power Transmission and Control, Qinhuangdao 066004, P. R. China)

Abstract

With many features, the magnetorheological fluid (MRF) damper is widely applied in the semi-active vibration control system. And sensitivity analysis is an important method to study the influence weight of various parameters on damping force characteristics. A mathematical model of the output damping force on the MRF damper is established by the mechanism modeling method, a first order output sensitivity equation is deduced and the expression of the first order output sensitivity function is obtained. The first-order sensitivity functions of ten design parameters are solved, and the influence degree of system parameters change on the output force of MRF damper is analyzed by comparing the sensitivity index of the parameters. Two sensitivities of vibration velocity and control current are obtained through experiment to prove the other parameters sensitivity analysis conclusion by analogy verification, which provides guidance for the structure optimization design of MRF damper.

Key words: magnetorheological fluid (MRF) damper, output damping force, first order sensitivity analysis, sensitivity index

0 Introduction

Vibration is a common phenomenon in the fields of general industry, aerospace, architecture, military and so on[1,2]. If not controlled effectively, vibration will seriously influence the lifetime and reliability of equipments. Therefore, study of vibration control is quite significant[3]. In recent years, with the rapid development of intelligent materials, more and more attention has been paid to realize semi-active vibration by using intelligent materials, such as MRF, with lots of application results.

The main damping material of a MRF damper is MRF. The damper has the advantages of simple structure, fast response speed, large control range of the damping force, adapting to the control of the wide frequency vibration, without excessive external energy access and with better control effect, so it is widely used[4]. Although overseas and domestic scholars have made great achievements in theoretical, rheological characteristics and technical applications of the MRF damper, research on the sensitivity of the output damping force to each design parameter is less. There are many factors that affect the output damping force of the MRF damper, including damper control current, piston motion velocity, turns of the excitation coil, the effective length of the piston and so on. According to the actual operating condition and structural parameter optimization theory, the influence mechanism of all parameters on the damping characteristics can be studied quantitatively[5]. However, the mathematical model of the MRF damper is so complex that it is difficult to obtain the influence of each parameter on the damping force accurately with the traditional method.

The sensitivity analysis method can be used to quantitatively analyze the influence weight of each parameter change on the characteristics of the system, so it is applied widely. Myung[6] proposed a sensitivity analysis method based on the finite element-transfer stiffness coefficient method and analyzed the free vibration sensitivity of a rectangular plates structure. Akihiro[7] obtained the intrinsic mode function sensitivity of continuum systems based on scalar Helmholtz equations. Then, they numerically optimized the 1D and 2D vibration problems to design the vibration resonator optimally. A time integration scheme of co-variance sensitivity has been proposed by Rita[8] to evaluate the

sensitivity analysis results of dynamic response with respect to structural parameters. Zhao[9] applied a sensitivity analysis method to the research on sensitivity of the mechanical vibration to the parameters in the vibration transmission path, then the vibration reduction design based on the structural parameters was carried out. Liao[10] applied the sensitivity analysis method to the optimal design of the frame structure of the cassava harvester and obtained the optimal design scheme of frame structure with the methods of fuzzy matter-element and entropy weight, improving the working performance. With the modal sensitivity theory, Zou[11] researched the modal sensitivity and mass sensitivity of the sheet metal and frame thickness and effectively solved the problem of severe vibration and noise. Based on the sensitivity analysis method, Guo[12] made a lightweight design of the machine tool mechanism to ensure the rigidity of the machine tool and reduce the manufacturing cost. Therefore, analyzing the damping force of the MRF damper with the sensitivity analysis method can obtain the influence weight of each parameter on the output damping force, which will provide guidance for the optimal design of the MRF damper.

MRF damper model is so complex that it is difficult to obtain the effect of each parameter on the output damping force. In order to solve this problem, firstly, the damping force mathematical model of the linear MRF damper is established in this paper. Then, based on the sensitivity analysis theory, the first order output sensitivity model of the output damping force is built. The first order output sensitivity functions about these structures or working parameters, such as the damper piston motion velocity and the control current, were set up. Next, numerical simulation was used to compare the influence of these parameters on the output damping force. Finally, piston motion speed and control current, the two parameters which are convenient to carry out experimental study, were selected to verify the accuracy of theoretical analysis.

1 Establishment of the first order output sensitivity model

In this paper, based on the Bingham model of MRF, the output damping force mathematical model of the MRF damper is established. The following assumptions are made in the modeling process:

1) The MRF is incompressible;

2) The working temperature of MRF ranges from $-40℃$ to $130℃$. The temperature has little effect on the damper performance, so it is not considered;

3) The MRF has low viscosity when the external

magnetic field strength is zero;

4) There is no residual magnetism in the core material, a small hysteresis loop area, low coercive force, no eddy current and hysteresis loss.

1.1 Flow analysis of MRF

Because of the small ratio between the flow gap and the diameter of the damper piston, one might conjectures that the axisymmetric flow field found in the damper can be approximated as flow through a parallel plate, as shown in Fig. 1.
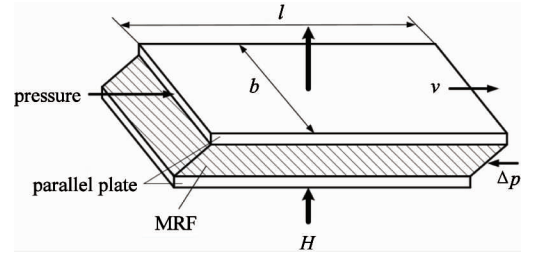

Fig. 1 The parallel plate model

In Fig. 1, l denotes the length of damping channel, b denotes the width of cross section, g denotes the gap between the two plates, ν denotes the relative velocity, Δp denotes pressure difference at the two ends of the damping channel.

In the plate model, the shear stress of MRF is linearly distributed along the plate gap. The flow can be divided into three regions[13]. In region ① and region ③, the shear stress exceeds the yield stress of MRF and begins to flow, called the yield zone. In region②, the shear stress is lower than the yield stress and is the rigid flow zone. The velocity distribution of MRF is shown in Fig. 2.
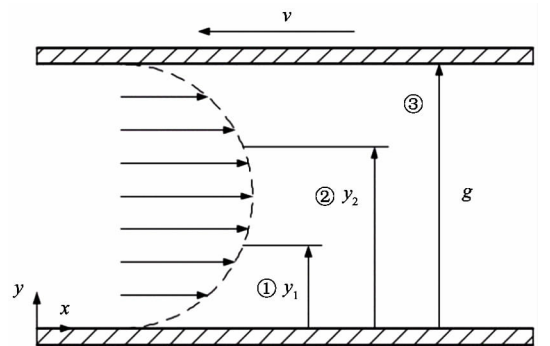

Fig. 2 Velocity distribution in the annular space

Based on the plane Poiseuille flow[14], the governing equation can be simplified as

$$\frac{\mathrm{d}\tau}{\mathrm{d}y} = \frac{\Delta p}{l} \tag{1}$$

The MRF is the Bingham fluid under the external

magnetic field. When MRF flows between the parallel plates, the expression is shown as

$$\begin{cases} \tau = \tau_y \, \text{sgn}(\dfrac{du}{dy}) + \eta \dfrac{du}{dy} & (\tau > \tau_y) \\ \dot{\gamma} = \dfrac{du}{dy} = 0 & (\tau < \tau_y) \end{cases} \tag{2}$$

where, τ is the fluid shear stress (Pa), τ_y is the hysteresis shear yield stress (Pa), η is the apparent viscosity coefficient of the MRF (Pa · s), $\dot{\gamma}$ is the shear strain rate of fluid (Pa/s).

The relationship between theoretical shear yield stress τ_y and magnetic induction intensity B can be approximated as

$$\tau_y = 152B - 11.4 \tag{3}$$

The flow velocity in the three regions are represented by u_1, u_2 and u_3 respectively, and the boundary conditions are as follows:

Region ①: $0 \leqslant y \leqslant y_1$, $\tau = \tau_y + \eta \dfrac{du_1}{du_2}$, $u_1(0)$

$= 0$, $\dfrac{du_1(y_1)}{dy} = 0$;

Region ②: $y_1 \leqslant y \leqslant y_2$, $\dfrac{du_2(y_1 < y < y_0)}{dy} =$

0, $\tau(y_1) = -\tau_y$, $\tau(y_2) = \tau_y$;

Region ③: $y_2 \leqslant y \leqslant g$, $\tau = -\tau_y + \eta \dfrac{du_1}{dy}$, $u_3(g)$

$= -v$, $\dfrac{du_3(y_2)}{dy} = 0$.

In region ①, τ is substituted into Eq. (1), the expression is shown as

$$\eta \frac{d^2 u_1}{dy^2} = \frac{\Delta p}{l} \tag{4}$$

Eq. (4) can be calculated according to the boundary conditions, and thus the flow velocity of region ① can be calculated as

$$u_1 = \frac{\Delta p}{2\eta l}(y^2 - 2y_1 y) \tag{5}$$

Similarly, the flow velocity of region ② is calculated as

$$u_2 = -\frac{\Delta p}{2\eta l} y_1^2 \tag{6}$$

and the flow velocity of region ③ is calculated as

$$u_3 = \frac{\Delta p}{2l\eta^2}(\eta y^2 - 2y_2 y + 2gy_2 - g^2\eta) - v \tag{7}$$

Based on Eq. (1) and the boundary condition $\tau(\dfrac{g}{2}) = 0$, the shear stress distribution of MRF is expressed as $\tau = \dfrac{\Delta p}{2l}(2y - g)$.

Considering that $\tau(y_1) = -\tau_y$ and $\tau(y_2) = \tau_y$, the expression is shown as

$$y_1 = \frac{g}{2} - \frac{l\tau_y}{\Delta p} \tag{8}$$

$$y_2 = \frac{g}{2} + \frac{l\tau_y}{\Delta p} \tag{9}$$

The thickness of rigid flow zone is expressed as

$$\delta = y_2 - y_1 = \frac{2l\tau_y}{\Delta p} \tag{10}$$

A non-dimensional factor is introduced as

$$\bar{\delta} = \frac{\delta}{g} = \frac{2l\tau_y}{g\Delta p} \tag{11}$$

Then Eq. (11) is substituted into Eqs (8) and (9) as

$$y_1 = \frac{g}{2}(1 - \bar{\delta}) \tag{12}$$

$$y_2 = \frac{g}{2}(1 + \bar{\delta}) \tag{13}$$

Q is the volume flow rate of MRF in the plate gap, which is expressed as

$$Q = \int_0^{y_1} bu_1 dy + \int_{y_1}^{y_2} bu_2 dy + \int_{y_2}^{g} bu_3 dy \tag{14}$$

where, $Q_1 = \displaystyle\int_0^{y_1} bu_1 dy = -\frac{\Delta p b y_1^3}{3l\eta}$

$Q_2 = \displaystyle\int_{y_1}^{y_2} bu_2 dy = -\frac{\Delta p b y_1^2 (y_2 - y_1)}{2l\eta}$

$Q_3 = \displaystyle\int_{y_2}^{g} bu_3 dy = \frac{\Delta p b}{2l\eta^2}(g - y_2)[\frac{1}{3}\eta(g^2 + gy_2$

$+ y_2^2) - y_2^2 + gy_2 - g^2\eta - \frac{2l\eta^2 v}{\Delta p}]$

where, $b = \pi(D + g)$

According to the continuity principle of fluid mechanics, the output damping force of the MRF damper is expressed as

$$F = -\Delta p A \tag{15}$$

And there is the following relation

$$Q = Av \tag{16}$$

where, A is the piston effect area, $A = \dfrac{(D^2 - d^2)\pi}{4}$.

1.2 Magnetic circuit analysis

When assuming that the damper core permeability is constant, and ignoring the magnetic flux leakage and friction loss, the relationship among the magnetic reluctance R_m, the flux φ and the magnetic potential F_f can be expressed as

$$F_f = R_m \phi \tag{17}$$

Magnetic potential F_f can be expressed as

$$F_f = NI \tag{18}$$

where, N is the coil turn's number, I is the field current.

The formula of magnetic induction intensity is

$$B = \mu H \tag{19}$$

where, B is the magnetic induction intensity, μ is the core permeability, H is the intensity of magnetic field (T).

The magnetic flux is expressed as

$$\phi = BS \tag{20}$$

where, S is the cross-sectional area of the iron core.

Considering from Eq. (17) to Eq. (20), the intensity of magnetic field is expressed as

$$H = \frac{NI}{\mu R_m S} \tag{21}$$

It is assumed that the average length of the magnetic circuit is $L(\mathrm{m})$, and the relative permeability is μ_R, the permeability of cylinder material is μ_0, so magnetic reluctance R_m can be expressed as

$$R_m = \frac{L}{\mu S} = \frac{l}{\mu_R \mu_0 S} \tag{22}$$

According to the structural characteristics of the damper iron core, the magnetic circuit is divided into three regions for analysis, as shown in Fig. 3.
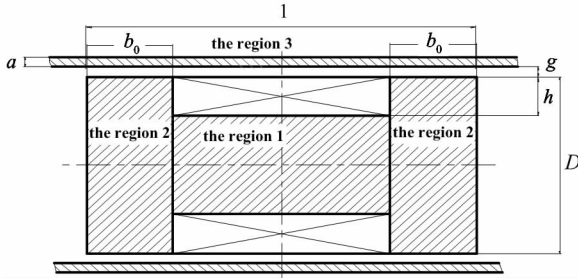

Fig. 3 Magnetic circuit of magnetizer

The three regions form a magnet, which makes up a closed magnetic circuit with the working gap. The coil current of the MRF damper consists of the field current and the iron loss current. At the low vibration frequency, the coil current can be seen as the field current, so the magnetic reluctance of each region is expressed as

$$R_{m_1} = \frac{l - 2b_0}{\frac{\pi}{4}\mu(D - 2h)^2} \tag{23}$$

$$R_{m_2} = \frac{D/2}{\mu D \pi b_0} = \frac{1}{2\mu\pi b_0} \tag{24}$$

$$R_{m_3} = \frac{l - b_0}{\mu_r \pi \left(D + g + \frac{a}{2}\right)a} \tag{25}$$

The magnetic reluctance of MRF can be approximated as

$$R_{MR} = \frac{\ln\left(1 + \frac{2g}{D}\right)}{2\mu_0\mu_{MR}\pi b_0} \tag{26}$$

where, μ_{MR} is the relative permeability of MRF, $\mu_{MR} =$

2.5.

The total magnetic reluctance is expressed approximately as

$$R_m = R_{m_1} + 2R_{m_2} + R_{m_3} + R_{MR} \tag{27}$$

In summary, the damping force formula is

$$H_3 F^3 + H_2 F^2 + H_1 F + H_0 = 0 \tag{28}$$

where,

$$H_3 = -\frac{\frac{9}{4}bg^3 - \frac{3}{2}\eta bg^3 - 6Avl\eta^2 - 3blgv\eta^2}{A^3}$$

$$H_2 = \frac{\frac{15}{4}bl\tau_y g^2 + \frac{13}{4}b\eta l\tau_y g^2 - \frac{3}{2}b\eta g^3 - 6bv\tau_y l^2\eta^2}{A^2}$$

$$H_1 = \frac{7\eta bgl^2\tau_y^2 + 9bgl^2\tau_y^2 - b\eta l^2\tau_y^2}{A}$$

$$H_0 = l^3\tau_y^3(b\eta - 2\eta + 3b)$$

1.3 Establishment of the first order output sensitivity model

This paper mainly analyzes the output sensitivity of the ten parameters related to the structure and working process of the MRF damper. The output sensitivity equation of each parameter is expressed as

$$\dot{\lambda}_\alpha = f(\alpha, t) \tag{29}$$

where, α is the parameter matrix, $\dot{\lambda}_\alpha$ is the first order sensitivity matrix of each parameter, and t is the time.

The parameter matrix is expressed as

$$\boldsymbol{\alpha} = [\alpha_1, \alpha_2, \alpha_3, \alpha_4, \alpha_5, \alpha_6, \alpha_7, \alpha_8, \alpha_9, \alpha_{10}]$$

where, α_1 is the control current of the MRF damper and α_2 is the piston motion velocity, which can affect the final output damping force, and the parameters can be adjusted according to actual conditions. Some parameters can affect the shear yield stress, and then affect the output damping force, such as the excitation coil turns α_3, the core cross-sectional area α_4, the core permeability α_5 and the apparent viscosity coefficient of the MRF α_6. In addition, the gap between outer cylinder and piston cylinder α_7, the piston damping ring diameter α_8, the piston shaft diameter α_9 and the piston effective length α_{10} can also affect the output damping force.

The first-order partial derivative of the parameters from damping force F in Eq. (28) is calculated. Then the first order output sensitivity function of each parameter can be obtained by MATLAB software programming. In the engineering application, the output damping force is controlled by adjusting the control current and the piston motion velocity in most cases[15]. Therefore, this paper focuses on the first order output sensitivity of control current and piston motion velocity.

The expressions of the control current and the pis-

ton motion velocity are expressed as

$$\dot{\lambda}_{\alpha_1} = \frac{\partial F}{\partial \alpha_1} =$$

$$\left[3A^3 l^3 \tau_y^2 (2\eta - b\eta - 3b)(\frac{I+e}{14580} + 1281) \right.$$

$$+ 2A^2 \tau_y F (7\eta b g l^2 + 9 b g l^2 - b\eta l^2)(\frac{I+e}{14580} + 1281)$$

$$\left. + AF^2 (\frac{15}{4} b l g^2 + \frac{13}{4} b\eta l g^2 - 6 b v l^2 \eta^2)(\frac{I+e}{14580} + 1281) \right]$$

$$\cdot \left[A^2 (7\eta b g l^2 \tau_y^2 + 9 b g l^2 \tau_y^2 - b\eta l^2 \tau_y^2) \right.$$

$$+ 2AF(\frac{15}{4} b l \tau_y g^2 + \frac{13}{4} b\eta l \tau_y g^2 - \frac{3}{2} b\eta g^3 - 6 b v \tau_y l^2 \eta^2)$$

$$\left. - 3F^2 (\frac{9}{4} b g^3 - \frac{3}{2} \eta b g^3 - 6 A v l \eta^2 - 3 b g l v \eta^2) \right]^{-1} \tag{30}$$

$$\dot{\lambda}_{\alpha_2} = \frac{\partial F}{\partial \alpha_2} =$$

$$\left[6 b \tau l^2 \eta^2 A F^2 - (6 A l \eta^2 + 3 b g l \eta^2) F^3 \right]$$

$$\cdot \left[A^2 (7\eta b g l^2 \tau_y^2 + 9 b g l^2 \tau_y^2 - b\eta l^2 \tau_y^2) \right.$$

$$+ 2AF(\frac{15}{4} b l \tau_y g^2 + \frac{13}{4} b\eta l \tau_y g^2 - \frac{3}{2} b\eta g^3 - 6 b v \tau l^2 \eta^2)$$

$$\left. - 3F^2 (\frac{9}{4} b g^3 - \frac{3}{2} \eta b g^3 - 6 A v l \eta^2 - 3 b g l v \eta^2) \right]^{-1} \tag{31}$$

The change in parameters $\Delta\alpha$ will cause the change ΔF of the output damping force. The first order Taylor expansion of the damping force is shown as

$$F(t, \alpha + \Delta\alpha) = F(t, \alpha) + (\frac{\partial F(t, \alpha)}{\partial \alpha}) \cdot \Delta\alpha$$
$$+ \text{ higher order items} \tag{32}$$

For a single parameter change $\Delta\alpha$, Eq. (32) can be expressed as

$$F(t, \alpha + \Delta\alpha_i) = F(t, \alpha) + (\frac{\partial F(t, \alpha_i)}{\partial \alpha_i}) \cdot \Delta\alpha_i$$
$$+ \text{ higher order items} \tag{33}$$

where, $\frac{\partial F(v, \alpha_i)}{\partial \alpha_i}$ is the first order output sensitivity function $\dot{\lambda}_{\alpha_i}$. Eq. (29) is substituted into Eq. (33) as

$$\Delta F = \dot{\lambda}_\alpha \cdot \Delta\alpha + \text{ higher order items} \tag{34}$$

Eq. (34) is the first order approximate expression of the output damping force change ΔF caused by parameter variation $\Delta\alpha$. First order output sensitivity function $\dot{\lambda}_{\alpha_i}$ of each parameter is calculated, then multiply it with the parameters change $\Delta\alpha$, so the output damping force variation ΔF caused by the parameters

change can be calculated.

2 Simulation analysis of the first order output sensitivity

2.1 Sensitivity function solution

Programs were written in MATLAB software based on the calculation of the first order output sensitivity equation. The output sensitivity function curve of the MRF damper output damping force is shown in Fig. 4.

It can be seen that the ten parameters will affect the change of output damping force. Some parameters have a great impact on the system dynamics and a relatively small effect on the system stability in the whole adjustment time, such as α_1, α_3, α_4, α_5, α_7, α_8 and α_9. These parameters tend to be stable at the end of the sampling time. The change of α_2 will cause the flow change, flowing from the high pressure chamber to the low pressure chamber in the damper, which results in the variation of the damping force. Changing α_6 will increase the output damping force at zero magnetic field intensity. With the increase of α_{10}, the length of the damping hole becomes larger and the damping force increases. The magnetic reluctance becomes larger and the intensity of magnetic field decreases, which leads to the decrease of the shear force. Therefore, the three parameters can consistently affect the steady state of the system and the system is ultimately not stable.

2.2 The sensitivity index

Two different sensitivity indexes are defined to quantify the influence of parameters α on damping force F intuitively.

The influence of each parameter on damping force F is measured by the output damping force variation $\triangle F$ of the MRF damper. Ignoring the higher order terms in Eq. (34), the expression can be described as

$$\frac{\Delta F_i}{F_{\max}} \times 100\% = \frac{\dot{\lambda}_{\alpha_i} \cdot \Delta\alpha_i}{F_{\max}} \times 100\% \tag{35}$$

The maximal value of this percentage is regarded as the peak sensitivity index and the result is expressed by s_1.

$$s_1 = \left. \frac{|\Delta F_i|}{F_{\max}} \right|_{\max} \times 100\%$$

$$= \left. \frac{|\dot{\lambda}_{\alpha_i}| \cdot \Delta\alpha_i}{F_{\max}} \right|_{\max} \times 100\% \tag{36}$$

(a) The first order output sensitivity function $\dot{\lambda}_{\alpha_1}$ (b) The first order output sensitivity function $\dot{\lambda}_{\alpha_2}$ (c) The first order output sensitivity function $\dot{\lambda}_{\alpha_3}$

(d) The first order output sensitivity function $\dot{\lambda}_{\alpha_4}$ (e) The first order output sensitivity function $\dot{\lambda}_{\alpha_5}$ (f) The first order output sensitivity function $\dot{\lambda}_{\alpha_6}$

(g) The first order output sensitivity function $\dot{\lambda}_{\alpha_7}$ (h) The first order output sensitivity function λ_{α_8} (i) The first order output sensitivity function λ_{α_9}

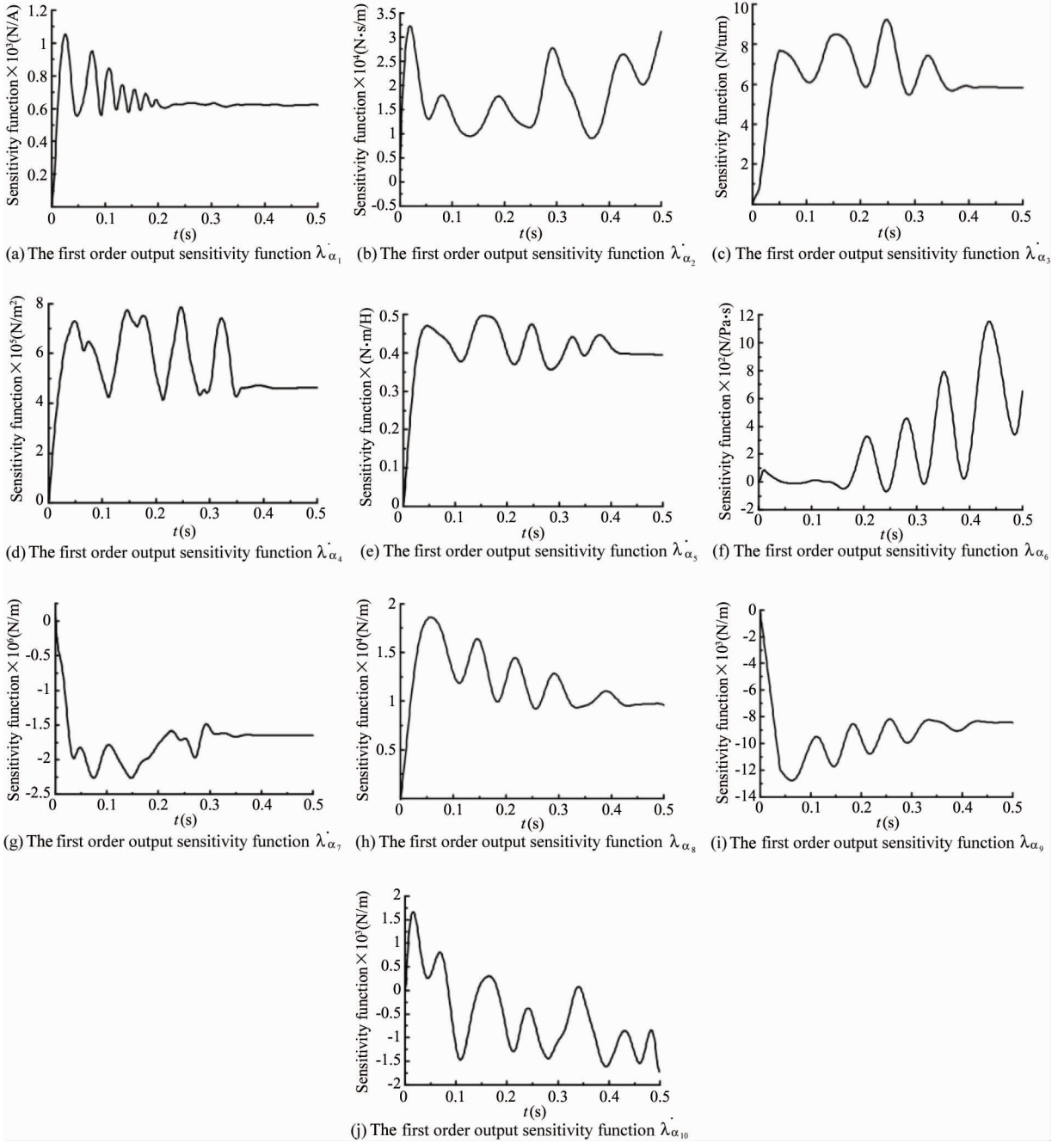(j) The first order output sensitivity function $\dot{\lambda}_{\alpha_{10}}$

Fig. 4   The sensitivity function curve of each parameter

In order to evaluate the overall level of influence of damper parameters on $\triangle F$, The integration for $|\dot{\lambda}_{\alpha_i}|$ · $\Delta\alpha_i$ in the sampling time is called the mean sensitivity index, which is expressed as s_2.

$$s_2 = \int_0^{t_0} |\dot{\lambda}_{\alpha_i}| \cdot \Delta\alpha_i dt \qquad (37)$$

2.3   Peak sensitivity and mean sensitivity analysis

According to Eq. (35), when each parameter change reaches 10%, the change percentage of the output damping force is shown in Fig. 5.
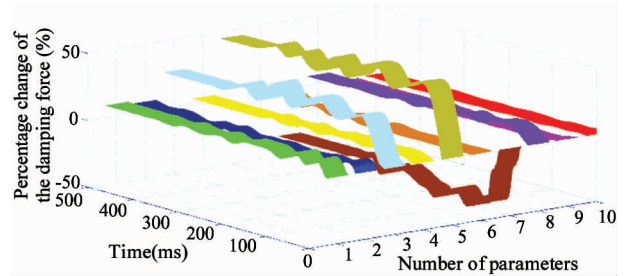

Fig. 5   The temporal curve of damping force change percentage caused by the parameters

The peak sensitivity index and the mean sensitivity index of each parameter are obtained by the first order output sensitivity analysis method, and the column is shown in Fig. 6.
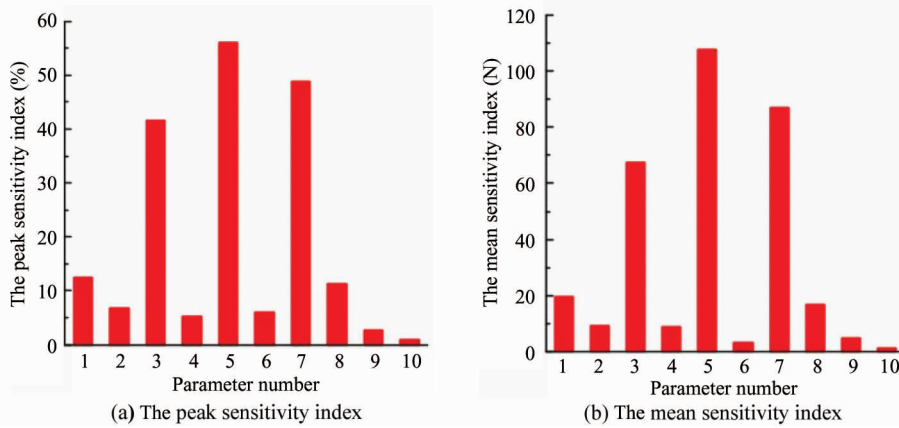

Fig. 6   Sensitivity index of each parameter

The conclusions are as follows:

1) The two sensitivities of these parameters, including α_2, α_4, α_6, α_9 and α_{10}, are relatively small. The peak sensitivity is less than 10% and the mean sensitivity is less than 10N. Therefore, these parameters have little effect on the output damping force when they vary 10%.

2) The sensitivity of α_1 and α_8 is larger. The peak sensitivity ranges from 10% to 15% and the mean sensitivity is close to 20N. It is shown that the influence of the two parameters change 10% on the output damping force is increased.

3) For some parameters, the peak sensitivity is greater than 40% and the mean sensitivity is greater than 60N, such as α_3, α_5 and α_7. The output damping force changes greatly when the three parameters change by 10%, so these parameters should be considered carefully in the design of the MRF damper.

4) The sensitivity of α_5 is the largest. It suggests that the parameter has great influence on the output damping force. In order to avoid the MRF damper damage caused by the excessive damping force, special attention should be paid to the core permeability in the selection of the core material.

3   Experimental study

The performance testing system of the experimental platform of MRF damper is shown in Fig. 7.

In this paper, the sensitivity of the piston motion velocity and the control current is studied experimentally. During the experiment, the control current and the piston motion velocity vary by 10% and 20% respectively. The experimental and simulation curves of first
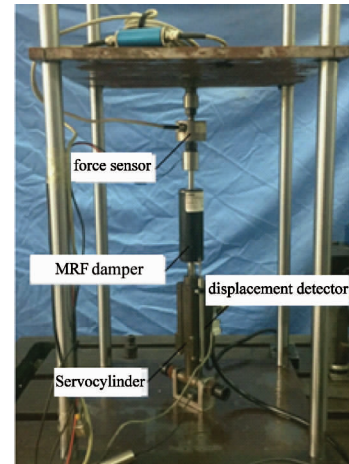

Fig. 7   The performance testing system experimental platform of MRF damper

order output sensitivity is shown in Fig. 8.

It can be seen that when the control current and the piston motion velocity change 10% and 20% respectively, the change trend is basically consistent with the simulation curve, even if there is a large fluctuation in the experimental curve. Therefore, the sensitivity analysis model and the analysis method established in this paper are accurate.

4   Conclusion

In order to solve the problem that it is difficult to obtain the influence of each parameter on the output damping force due to the complex model, the study is carried out based on a linear MRF damper. The effect of the structural parameters and operating parameters on the output damping force is studied by using the first order sensitivity analysis method numerically and
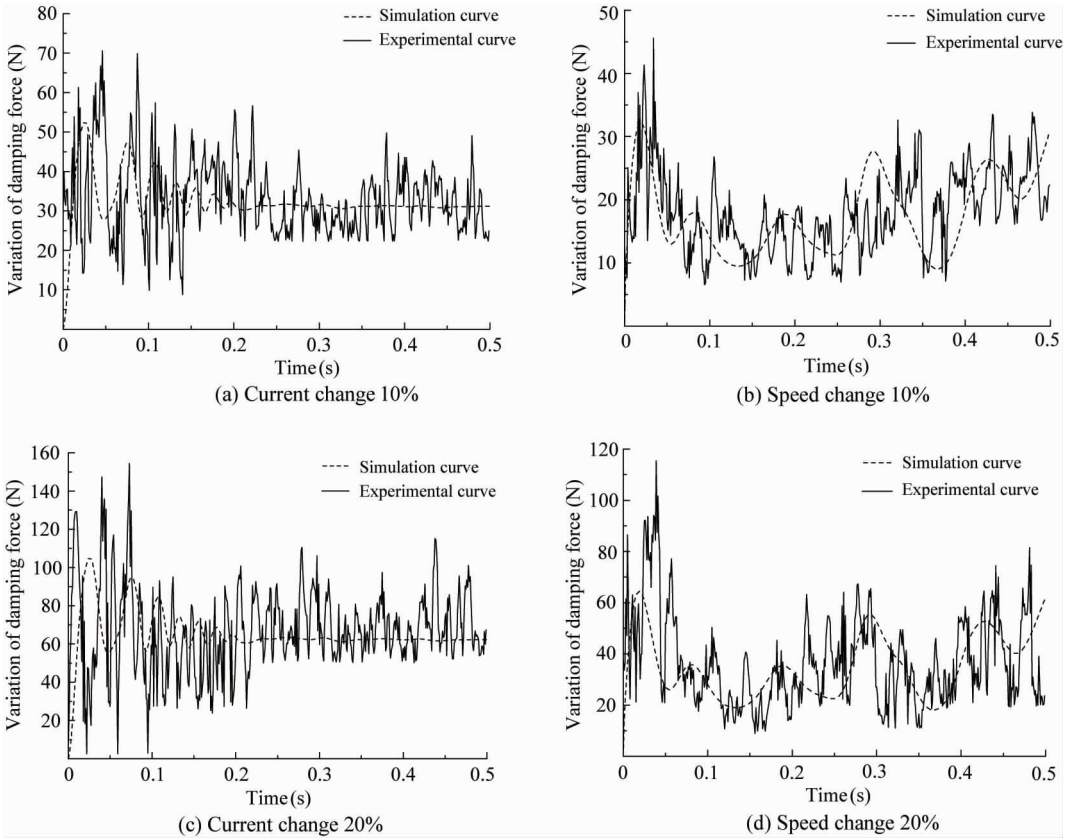
Fig. 8   The curve of simulation compared with the experiment

experimentally. The conclusions are as follows:

(1) The parameters have influence on the output damping force, but the weight of the parameters is different. The parameters include control current, piston motion velocity, excitation coil turns, core cross-sectional area, core permeability, the apparent viscosity coefficient of the MRF, the gap between outer cylinder and cylinder, piston damping ring diameter, piston shaft diameter and piston effective length.

(2) In the experiment, the change trend of damping force is studied when the control current and the poison speed vary at 10% and 20% individually. The control current change makes the damping force tend to be stable, and the variety of the piston motion velocity makes it change continuously. The first order sensitivity analysis is similar to the experiment results, which proves that the first order sensitivity model and the analysis method are correct.

(3) Parameters have different influence on the damping force. The excitation coil turns, the core permeability and the gap between outer cylinder and cylinder have the most influence on the damping force, the control current and the piston damping ring diameter take second place. The piston motion velocity, the core cross-sectional area, the apparent viscosity coefficient of the MRF, the piston shaft diameter and the piston effective length have little influence on the damping force.

References

[1] Li S W, Zhang G X. Development status quo of modern hydraulic technology. *Mechanical Engineer*, 2009,2: 54-57 (In Chinese)

[2] Quan L X, Kong X D, Yu B, et al. Research status and trends on fluid-structure interaction vibration mechanism and control of hydraulic pipeline. *Journal of Mechanical Engineering*, 2015, 51(18): 1-6

[3] Liu W, Liu Y S, Jiang Z F, et al. Pulsation reliability analysis of hydraulic power pipelines. *Journal of Vibration and Shock*, 2011, 30(6): 265-268

[4] Mazlan S A, Ismail I, Zamzuri H, et al. Compressive and tensile stresses of magneto-rheological fluids in squeeze mode. *International Journal of Applied Electromagnetics and Mechanics*, 2011, 36(4): 327-337

[5] Jia W H, Yin C B, Cao D H. Optimization of hydraulic spool valve based on AMESim/MATLAB. *Machine Tool & Hydraulics*, 2013, 41(15): 182-183

[6] Myung S C, Jung H B. Sensitivity analysis for free vibration of rectangular plate. *Journal of Sound and Vibration*, 2013, 332(6): 1610-1625

[7] Akihiro T, Mitsuru K. Sensitivity analysis and optimization of vibration modes in continuum systems. *Journal of Sound and Vibration*, 2013, 332(6): 1553-1566

[8] Rita G, Francesco T. Structural reliability sensitivities under nonstationary random vibrations. *Mathematical*

Problems in Engineering, 2013: 69-90

[9] Zhao J, Li F, Liu L. Vibration characteristic sensitivity analysis based on finite element for ultra-high pressure pipeline systems. *Journal of Vibration and Shock*, 2014, 33(10): 148-151

[10] Liao Y L, Liu S H, Sun Y P, et al. Structural optimization for rack of cassava harvester based on sensitivity analysis. *Transactions of the Chinese Society for Agricultural Machinery*, 2013, 44(12): 56-61

[11] Wu G M, Shi W K, Liu W, et al. Structural optimization of a light bus body-in-white based on model sensitivity analysis. *Journal of Vibration and Shock*, 2013, 32(3): 41-45

[12] Guo L, Zhang H, Ye P Q, et al. Light weight design of machine tool based on sensitivity analysis. *Journal of Tsinghua University (Science and Technology)*, 2011, 51(6): 846-850

[13] Ma R, Zhu S H, Liang L, et al. Modelling and testing of magnetorheological damper. *Journal of Mechanical Engineering*, 2014, 50(4): 135-141

[14] Cao J G, Fu L J, Deng G H, et al. Mechanical properties analysis of automobile magnetorheological fluid absorber. *Mining & Processing Equipment*, 2005, 33(8): 41-44

[15] Yang Z, Zhu C, Zheng J J, et al. Magnetic field response time analyses in magneto-rheological damper and correction circuit design. *Machine Tool & Hydraulics*, 2013, 41(5): 22-25

Kong Xiangdong, born in 1959, Eng. D. professor. He received his Eng. D degree from Yanshan University in 1991 and his Ph. D and M. E. degrees from Yanshan University in 1985. He also received his B. E. degree from Zhejiang University in 1982. He is the Vice President of Yanshan University and the Director of Hebei Provincial Key Laboratory of Heavy Machinery Fluid Power Transmission and Control. His research focures on electro-hydraulic servo control system.